Understanding the Cytochrome *c* Oxidase Proton Pump: Thermodynamics of Redox Linkage

Siegfried M. Musser and Sunney I. Chan
Arthur Amos Noyes Laboratory of Chemical Physics, California Institute of Technology, Pasadena, California 91125 USA

ABSTRACT The cytochrome *c* oxidase complex (CcO) catalyzes the four-electron reduction of dioxygen to water by using electrons from ferrocytochrome *c*. Redox free energy released in this highly exergonic process is utilized to drive the translocation of protons across a transmembrane electrochemical gradient. Although numerous chemical models of proton pumping have been developed, few attempts have been made to explain the stepwise transfer of energy in the context of proposed protein conformational changes. A model is described that seeks to clarify the thermodynamics of the proton pumping function of CcO and that illustrates the importance of electron and proton gating to prevent the occurrence of the more exergonic electron leak and proton slip reactions. The redox energy of the CcO-membrane system is formulated in terms of a multidimensional energy surface projected into two dimensions, a nuclear coordinate associated with electron transfer and a nuclear coordinate associated with elements of the proton pump. This model provides an understanding of how a transmembrane electrochemical gradient affects the efficiency of the proton pumping process. Specifically, electron leak and proton slip reactions become kinetically viable as a result of the greater energy barriers that develop for the desired reactions in the presence of a transmembrane potential.

INTRODUCTION

The cytochrome *c* oxidase complex (CcO) is the terminal electron transport protein complex of the respiratory chain in eukaryotes and most prokaryotes. This integral membrane protein catalyzes the reduction of dioxygen to water by using four electron equivalents from ferrocytochrome *c*. Eukaryotic CcO contains four redox-active metal centers, two copper sites (Cu_A and Cu_B), and two heme A sites (cytochrome *a* and cytochrome a_3). Cu_A and cytochrome *a* are the initial electron acceptors from cytochrome *c* whereas Cu_B and cytochrome a_3 form a binuclear center and together compose the site of dioxygen activation and reduction. A portion of the free energy released from the highly exergonic reduction of dioxygen is used to drive the transport of protons from the matrix to the intermembrane space against a transmembrane electrochemical gradient (Chan and Li, 1990; Malmström, 1990; Babcock and Wikström, 1992). It has been experimentally determined that the proton pumping stoichiometry is approximately 1 H^+/e (Wikström, 1977; Wikström and Krab, 1978; Casey et al., 1979; Sigel and Carafoli, 1979; van Verseveld et al., 1981; Solioz et al., 1982; Proteau et al., 1983); however, the four protons are ejected only during the second half of the turnover cycle (Wikström, 1989). Despite steady progress on this problem over the years, the molecular mechanism of the proton pumping process has remained elusive. Although the electron transfer (ET) pathways within the enzyme complex are slowly becoming clear, there is still no consensus on which of the four redox sites is (are) most intimately involved in redox linkage. In fact, each of the four redox centers has been postulated to play a central role in the proton pump mechanism, and fairly detailed models have been presented for each case (Babcock and Callahan, 1983; Gelles et al., 1986; Larsen et al., 1992; Rousseau et al., 1993; Woodruff, 1993; Wikström et al., 1994). In all scenarios, however, it is accepted on faith that the required conformational changes are linked to loss of redox energy. In particular, no attempt has been made to assess the energetic requirements of the proposed conformational changes as they relate to enzyme turnover. We demonstrate here such a description of the proton pump and illustrate that this exercise leads to considerable insight into the coupling between the electron and proton transfer reactions.

Received for publication 14 November 1994 and in final form 27 March 1995.

Address reprint requests to Dr. Sunney I. Chan, California Institute of Technology, Mail Code 127–72, Pasadena, CA 91125. Tel.: 818-395-6508; Fax: 818-578-0471; E-mail: chans@starbase1.caltech.edu.

0006-3495/95/06/2543/13 $2.00

DISCUSSION

Energetics of the catalytic cycle

In the resting enzyme, cytochrome *a*, cytochrome a_3 and Cu_A have been found to have reduction potentials of approximately 340, 290, and 290 mV, respectively, at room temperature and pH 7 (Blair et al., 1986; Wang et al., 1986). The lack of spectroscopic signals for Cu_B has hindered direct experimental investigation of its redox properties, but it is generally assigned a reduction potential of approximately 340 mV (Brunori et al., 1987). These midpoint potentials are difficult to define as they vary during turnover as electrons are input to the enzyme (complicating the reduction potential measurements themselves) and as the binuclear center is activated by dioxygen (see below). For example, it has been estimated that the two hemes have approximately equal reduction potentials (340–360 mV) in the fully oxidized enzyme, yet when one heme is reduced, the reduction potential of the remaining heme drops to 220–250 mV (Brunori et al., 1987). Nevertheless, these potentials provide a convenient

point of departure for the present discussion. The midpoint potential of cytochrome *c* is approximately 250 mV (Rodkey and Ball, 1950), implying that the maximal redox free energy available from electron input from cytochrome *c* to fully oxidized CcO under standard conditions is approximately 90 mV (ET from cytochrome *c* to cytochrome *a* or Cu_B). In respiring mitochondria, however, the electrochemical potential barrier to proton transfer across the inner mitochondrial membrane (the proton motive force or pmf) is approximately 200 mV (Rottenberg, 1979; Wikström and Saraste, 1984), indicating that proton pumping is unlikely to occur upon electron input to fully oxidized CcO. On the other hand, the situation changes dramatically when the binuclear center is activated by formation of the two- and three-electron reduced dioxygen intermediates (compound C and oxyferryl, respectively). From experiments on the reversal of the catalytic cycle of CcO by high concentrations of ATP, it was estimated that these intermediates have reduction potentials of approximately 940 (compound C) and 800 (oxyferryl) mV (Wikström, 1988). Recently, these estimates have been revised upwards to 1.22 and 1.05 V, respectively (Wikström and Morgan, 1992). In any case, the strong oxidizing ability of dioxygen substantially raises the reduction potential of the binuclear site when dioxygen binds to the enzyme. Dioxygen does not appear to bind to CcO until at least two electrons have been input to the enzyme (Brezezinski and Malmström, 1987; Fabian et al., 1987). Thus, proton pumping can occur only upon transfer of the third and fourth electrons to the activated binuclear center during the dioxygen reduction cycle. Given that the overall stoichiometry of the CcO proton pump is approximately 1 H^+/e^- and the first two electrons of the dioxygen reduction cycle are not coupled to proton pumping, the average stoichiometry for the third and fourth electrons must then be 2 H^+/e^-. We note that this picture, in which the electrons involved in dioxygen reduction are inequivalent with respect to the proton pump, has been proven experimentally by poising cytochrome *c* at a high reduction potential and partially reversing the catalytic cycle of CcO in rat liver mitochondria (Wikström, 1988, 1989; Wikström and Morgan, 1992).

At pH 7, 35°C, and 0.05 atm O_2 (approximate physiological conditions in muscle (Myslovatyi et al., 1982)), the O_2/H_2O and O_2/H_2O_2 redox couples have potentials of approximately 780 and 210 mV ($[H_2O_2]$ = 1 M), respectively, in aqueous buffers. As the reduction potentials of the redox centers of fully oxidized CcO are ≥290 mV, it is clear that the O_2/H_2O_2 redox couple involved in CcO turnover must function at a higher potential for efficient formation of compound C. In fully energized mitochondria, $\Delta\psi$ is approximately 150 mV (Rottenberg, 1979). Therefore, as two charge-equivalents traverse the inner mitochondrial membrane during the dioxygen reduction process, the O_2/H_2O_2 couple must minimally function at approximately 290 mV + 150 mV = 440 mV. (The electrons donated from cytochrome *c* do not traverse the entire membrane during the dioxygen reduction process; however, it is generally assumed that two protons are taken up by the binuclear center from the matrix upon formation of compound C. If this is so, the overall process is energetically equivalent to the inward transfer of two negative charge-equivalents across the inner mitochondrial membrane.) To drive the forward reactions and prevent reversibility, an additional 50–100 mV of redox free energy is likely required. Thus, the O_2/H_2O_2 couple probably functions at ≥500 mV. The low physiological concentration of H_2O_2 (micromolar range) and the increased stability of the H_2O_2-protein adduct (relative to free H_2O_2) are both expected to contribute to increasing the O_2/H_2O_2 potential to this level. The necessary consequence of this analysis is that the H_2O_2/H_2O couple must function at $2 \times \sim 780$ mV − 500 mV = ~1060 mV [$2 \times E^{red}(O_2/H_2O) - E^{red}(O_2/H_2O_2) = E^{red}(H_2O_2/H_2O)$], which agrees well with the estimates from Wikström's laboratory (Wikström, 1988; Wikström and Morgan, 1992). This result implies that an average of 1060 meV − 290 meV = 770 meV of free energy is available for the translocation of two protons and one electron across the fully charged mitochondrial membrane for the last two electrons of the catalytic cycle of CcO. As the net electron and proton transfer reactions occur in opposite directions across the membrane, both reactions are endergonic in the presence of a pmf. As a result, the transfer of a negative charge-equivalent across a fully charged mitochondrial membrane requires approximately 150 meV ($\Delta\psi$ = ~150 mV), and the transfer of two protons against the proton motive force (pmf = $\Delta\psi - 2.303(RT/F)\Delta pH$) requires $2 \times \sim 200$ meV = ~400 meV (Wikström and Saraste, 1984; Rottenberg, 1979). (Again, the electrons do not traverse the entire membrane during the dioxygen reduction process; however, proton uptake from the matrix is required as part of the dioxygen chemistry. This overall process is energetically equivalent to the inward transfer of a negative charge-equivalent across the inner mitochondrial membrane.) Under conditions of maximal pmf, then, a thermodynamic requirement of approximately 550 mV is required to pump two protons. The redox energy available to drive the ET steps and the conformational dynamics of the proton pump is therefore 770 mV − 550 mV = 220 mV, on average, for the third and fourth electrons of the catalytic cycle. Note that the $H_2O_2/H_2O_2^-$ and $H_2O_2^-/H_2O$ redox couples are expected to function at slightly different reduction potentials with the former functioning at the higher reduction potential (Wikström, 1988; Wikström and Morgan, 1992).

Requirements of a redox-linked proton pump

The energy released during the highly exergonic reduction of dioxygen must be transferred from the energetic electron to the protein matrix through a process that necessarily involves communication between at least one of the enzyme's redox centers and the proton-translocating elements. This process is termed redox linkage, and the redox center(s) involved in this transfer of energy to the polypeptide is(are) referred to as the site(s) of linkage. There are two distinct electronic states of a linkage site (oxidized and reduced). In addition, a number of distinct conformational substates (≥2) must ex-

ist for each of these electronic states; the appropriate cyclic conversion between these conformational states results in proton pumping. The efficacy of the proton pump relies heavily on electron and proton gating mechanisms. Electron gating refers to the requirement that the electron enters the linkage site in a different protein conformation than when it is transferred from this site. Similarly, proton gating implies that protons are input to the proton pump in a different conformation than that in which they are ejected (Chan and Li, 1990). These conformational changes are necessary to prevent reverse electron and proton transfers (according to the law of microscopic reversibility) as well as for dictating when subsequent reactions should occur. Thus, there are four requirements for a redox-linked proton pump: (1) a sufficiently exergonic ET, (2) redox linkage, (3) electron gating, and (4) proton gating. Clearly, the regulation of rates of ET and proton flow so that uncoupling reactions do not occur is fundamental to the efficiency of the proton pump. In fact, the most likely way that the enzyme can control the coupling of ET events to proton pumping is through kinetic control of ET pathways.

Energetics of redox linkage

There are several ways in which redox linkage could be achieved once the proton pump is engaged. In all scenarios, the site of linkage exists in at least two stable conformations, a stable oxidized configuration and a stable reduced configuration. The conversion between these two conformations results from oxidation/reduction of the site, and this conformational change is linked to conformational changes of the proton-translocating elements (redox linkage). Note that, for the majority of redox sites in proteins, the protein fold is so strong that minimal ligand rearrangement occurs upon a change in oxidation state, a condition that is ideal for efficient ET as a result of the low reorganizational energy (Williams, 1990). For blue copper proteins (such as azurin), the purpose of which is to act as electron carriers, the ligand configuration is intermediate between that preferred by Cu(II) and Cu(I). The protein fold is so strong (rack energy) that very little structural rearrangement occurs upon oxidation or reduction (Malmström, 1994). The linkage site in CcO, then, represents an exception to this general characteristic of electron transport proteins; in fact, ligand rearrangement is required for proton pumping to be feasible. Initially, oxidation/reduction of the linkage site results in a thermally unstable conformation of the protein; subsequent thermal relaxation allows the linkage site to adopt the more stable conformation. Clearly, the unstable and stable conformations of the oxidized/reduced linkage site are of different total energy. These conformational states of the enzyme can be represented by multidimensional vibronic potential energy wells. As the conformational coupling between a thermally unstable conformation and its associated stable conformation must be strong for an efficient proton pump (strong coupling is synonymous with efficient redox linkage), these two states can be represented by a single vibrational energy curve with two minima of different energies. The specific vibrational curve describing the energy state of the enzyme depends, of course, on the redox state of the linkage site. An exergonic ET from the linkage site is the process whereby the enzyme makes a transition from one vibronic potential curve to the other.

In Fig. 1, we illustrate various types of redox linkage for the case in which there is no pmf. Electrons are input to the linkage site from an electron donor (cytochrome *c* is used for simplicity), resulting in a thermally unstable conformation, $(cD^-A)_1$. Upon thermal relaxation, the enzyme achieves a lower energy conformational state, $(cD^-A)_2$. ET from $(cD^-A)_2$ to the activated binuclear site results in a different electronic state of lower energy, $(cDA^-)_2$. This state has an alternative nuclear configuration other than $(cD^-A)_2$, as the dioxygen intermediate present at the binuclear site is now one electron reduced. Again, the enzyme's conformation is described by a higher vibrational energy well; conformational

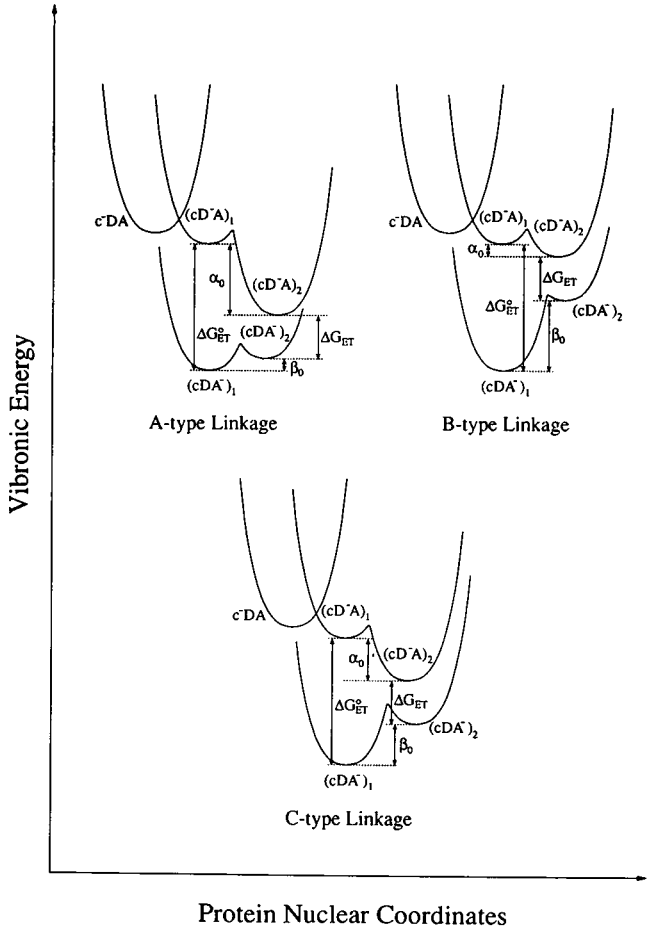

FIGURE 1 Schematics of A-, B-, or C-type redox linkage in the absence of a transmembrane potential. c denotes the primary electron donor to the linkage site (e.g., cytochrome *c*), D denotes the electron donor for the ET coupled to the proton pump (i.e., the linkage site), and A represents the compound C or oxyferryl dioxygen intermediate (electron acceptor). These symbols are used in unison (e.g., c^-DA) to denote a specific redox and conformational state of CcO. Plotted along the ordinate is the total vibronic energy of the enzyme complex, the electron-donating cytochrome *c*, and the protons involved in the dioxygen chemistry and the proton-pumping process. See text for further details.

relaxation allows the enzyme to achieve a nuclear configuration similar to the original electron input conformation, $(cDA^-)_1$. The conformational relaxations that occur when the linkage site is reduced or oxidized are described by the energy differences α_0 and β_0, respectively (both are negative quantities as defined here). The sum $|\alpha_0 + \beta_0|$ is the energy available to drive the proton pump; this energy is lost mostly as heat in the absence of a pmf. If redox linkage were nonexistent, the ET reaction would be described by ΔG°_{ET} (<0); however, as a result of coupling to the proton pump, the ET is described by $\Delta G_{ET} = \Delta G^\circ_{ET} - (\alpha_0 + \beta_0)$. This analysis implies that the internal ET is governed by only a fraction of the driving force available, and thus it is not necessary to invoke ET in the inverted region for the highly exergonic reduction of dioxygen.

The magnitude of the α_0 term represents the free energy available to prime the proton pump, that is, the energy the protein can access to achieve a conformation for which ejection of a proton across the chemiosmotic barrier is imminent. The magnitude of the β_0 term represents the free energy available to replenish the proton pump, that is, the energy the protein can utilize to take up a proton from the matrix and fill the hole created by the ejection of a proton into the intermembrane space. Both of these functions are required for any proton pump, but the relative magnitudes of α_0 and β_0 can vary significantly, depending on the energetic requirements of the chemical mechanism. For clarity, three cases are considered here: (1) $\alpha_0 > \beta_0$, which we will refer to as A-type linkage (Fig. 1 *A*); (2) $\alpha_0 < \beta_0$, which we will refer to as B-type linkage (Fig. 1 *B*); and (3) $\alpha_0 \approx \beta_0$, which we will refer to as C-type linkage (Fig. 1 *C*). Note that both α_0 and β_0 must be <0; in fact, for an efficient proton pump, $|\alpha_0|$ and $|\beta_0|$ must be large enough to drive the conformational changes irreversibly in a kinetically facile manner.

In addition, $\alpha_0 < 0$ implies that the effective reduction potential of D increases upon conversion from the $(cD^-A)_1$ state to the $(cD^-A)_2$ state; similarly, $\beta_0 < 0$ implies that the effective reduction potential of A increases upon conversion from the $(cDA^-)_2$ state to the $(cDA^-)_1$ state. Assuming that $D = Cu_A^{2+}$, this model implies that the reduction of Cu_A results in an increase in the reduction potential of this redox site. This change in reduction potential could occur by a ligand rearrangement or a ligand exchange reaction. However, the Cu_A site must communicate with A (the compound C or oxyferryl dioxygen intermediate) so that, upon reduction of Cu_A, the reduction potential of A decreases. Perhaps the simplest manner in which the reduction potential of A can be influenced is through the introduction of strain in the Fe_{a3}-His bond; however, polypepetide interactions with the bound dioxygen intermediate or perturbations to the heme macrocycle are also possible. Relaxation of A back to a conformation of higher reduction potential results upon ET from D to A. This discussion makes it clear that a given redox center is not the proton pump; rather, the whole protein is the proton pump. Thus, it may be difficult to identify the site of linkage by the simple observation of a conformational change at a given redox center; instead, cause and effect must be determined. The energetics of all conformational changes must be estimated for an accurate conclusion regarding the type of linkage.

In Fig. 2, a more complete representation of C-type linkage is depicted. We surmise that this type of redox linkage is the most general. To clarify our schematics, we have expanded the description of the protein's conformational space into two dimensions (instead of one as in Fig. 1). The vibronic energy is plotted along the *z*-direction whereas the *x* and *y* coordinates can be thought of as the nuclear coordinate associated with electron transfer (NCET) and the nuclear coordinate associated with the conformational elements of the proton pump (NCPP), respectively. In Fig. 2 *A*, the intersections of two planes ($x = x_1$ and $x = x_2$) with the protein's vibronic energy surface are shown. Each of these intersections is a two-dimensional potential energy curve with two wells labeled with the nomenclature introduced earlier. Potential energy curves along the *x* dimension are shown in Fig. 2, *B* and *C*. Although the potential energy curves are assumed to be parabolic along both the NCET and the NCPP, the coupling between the vibronic (conformational) states is of a different type and strength. Along the NCET, the coupling between the wave functions of the different electronic states is relatively weak and is governed by the electronic coupling matrix element, $[H_{ab}]$, according to the traditional theory of long-distance ET in proteins (Bowler et al., 1990; Marcus and Sutin, 1985). In contrast, along the NCPP, the coupling between nuclear configurations must be strong (for example, it would be virtually impossible to have a high energy $(cD^-A)_2$ conformation described by (x_1, y_1) as the enzyme simply denatures). Thus, along the NCET, the full parabolic nature of the two vibronic states is shown, whereas, along the NCPP, vibronic energy curves with two parabolic minima are depicted. This rationale explains the two-dimensional representations of redox linkage shown in Fig. 1, in which the weak electronic coupling between c^-DA and $(cD^-A)_1$ is explicitly depicted. It should be noted that the minimal energy of each vibronic state likely does not have an *x* or *y* coordinate in common with any other state. Thus, the minima depicted may not necessarily represent the true minima of the vibronic/conformational states represented. Nevertheless, it is useful to assume that the minima represented are the true minima to more accurately visualize free energy differences in these types of figures.

Review of the Chan Cu_A model

The Chan Cu_A model of redox linkage contains all of the elements essential for an efficient proton pump. The involvement of Cu_A in proton pumping has been questioned as the ubiquinol terminal oxidases, which are similar structurally, lack the Cu_A redox center yet still catalyze proton translocation (Babcock and Wikström, 1992; Trumpower and Gennis, 1994; Calhoun et al., 1994; van der Oost et al., 1994). An alternative proton translocation mechanism for the ubiquinol oxidases has been postulated, however (Musser et al., 1993a,b). As we are most familiar with the Chan Cu_A

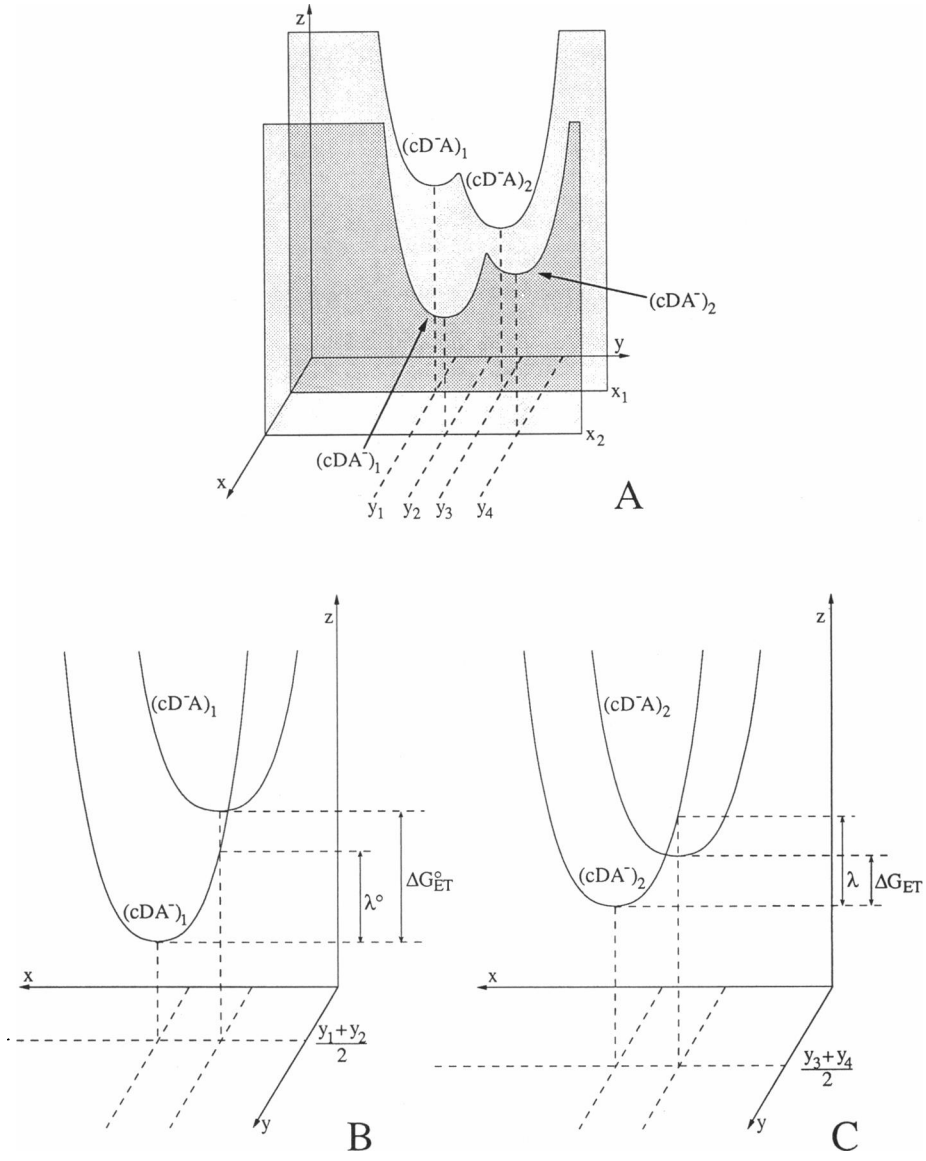

FIGURE 2 A model of C-type redox linkage in the absence of a transmembrane potential explicitly showing the NCET (x) and the NCPP (y) of the protein's vibrational energy surface. Vibronic energy is plotted along the z-direction.

model of redox linkage, we will further expand the above ideas on the thermodynamics of redox linkage in the framework of this model. The concepts we have developed here are completely general and are applicable to any molecular model of redox linkage proposed for CcO. First, however, we briefly review the ligand exchange reactions of the Chan Cu_A model.

Fig. 3 summarizes the postulated ligand exchange reactions of the Chan Cu_A model (Gelles et al., 1986). Cu_A^{2+} is assumed to be ligated by two histidines and two cysteine residues in a distorted tetrahedral arrangement; this is the electron input state (A). Upon reduction by ET from ferrocytochrome c, the Cu_A center becomes thermodynamically unstable (B). This thermodynamic instability results in a lengthening of one of the Cu-Cys bonds and, concurrently, a shortening of the distance between the copper ion and another ligand that is proposed to be a tyrosine (another residue with a similar pK_a is also possible) as in C. Eventually, full ligand exchange occurs via an S_N2-like mechanism, and the phenolic proton from the tyrosine is transferred to the dissociated thiolate anion (D). The ligand geometry is now roughly trigonal planar, the tyrosine pulling the copper slightly out of the plane formed by the other three ligands. ET to the activated binuclear site again results in a thermodynamically unstable conformation (E) prompting the reverse ligand exchange back to the original ligand structure. However, as a result of the greater charge on Cu_A in E than in C, transfer of the thiol proton back to the tyrosinate anion is inhibited, and, instead, this proton is released into a proton channel leading to the cytosolic side of the membrane (F). The tyrosine residue is reprotonated via a proton from a water or proton channel leading from the matrix (G). The loss of the thiol proton and the reprotonation of the tyrosinate anion may not occur simultaneously; hence, the two individual steps F and G.

Electron and proton gating mechanisms are incorporated in this model. ET from ferrocytochrome c to Cu_A^{2+} is faster in A than in E. Likewise, ET from Cu_A^{1+} to the activated

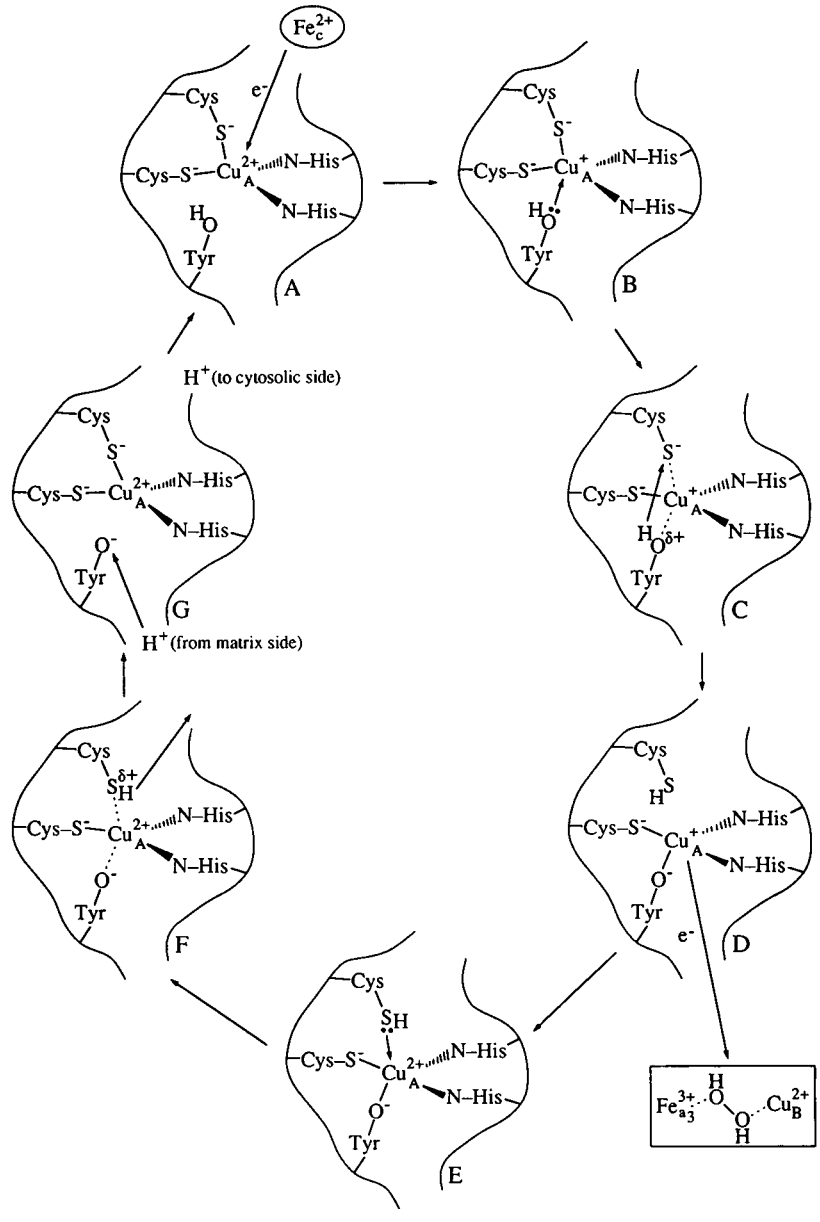

FIGURE 3 Chan Cu_A model of redox linkage. An expanded version of the model presented by Gelles and co-workers (1986). See text for details.

binuclear center is faster in *D* than in *B*. Gelles and co-workers (1986) estimated that Cu_A moves by a minimum of 3 Å, thus favoring the coupled ET over the uncoupled ET by a factor of at least 66. This motion of Cu_A allows for control of the desired ET by distance. There is another manner in which ET rates can be controlled in this model, however. By assuming that the major electron input pathway proceeds through the cysteine sulfur that dissociates from the Cu_A site ($B \rightarrow D$) and the major electron output pathway proceeds through the oxygen of the tyrosine, efficient electron gating is achieved by the creation and destruction of ET pathways. It is a little more difficult to envision how gating of proton flow occurs during this ligand exchange process as the transition state (approximately trigonal bipyramidal) appears identical in both the forward and reverse ligand exchange reactions. The transition states are not exactly identical, however, as the oxidation state of the redox site is different. Gelles and co-workers (1986) postulate that the greater charge on Cu_A in the $E \rightarrow A$ transition prevents transfer of the thiol proton back to the tyrosinate anion as a result of electrostatic repulsion but no insight into exactly how this occurs is provided. We suggest that the greater charge of the redox site directly affects the orientation of the incoming thiol ligand. This orientational effect has been incorporated into the model in Fig. 3; whereas the thiol proton is on the left side of the sulfur atom in *D*, it is on the right side in *E*.

This model assumes that ET proceeds from the Cu_A site to the activated binuclear center as the energy required for the proton pumping process must be coupled to the reduction of dioxygen. Recent evidence suggests that the Cu_A site, instead of cytochrome *a*, is the electron input site for the first electron (Hill, 1991, 1994; Oliveberg and Malmström, 1991; Pan et al., 1991; Stowell et al., 1993). These data indicate that

the first electron follows a cytochrome $c \rightarrow Cu_A \rightarrow$ cytochrome $a \rightarrow$ binuclear center pathway. Few data are available that directly address electron input for the third and fourth electrons, however. The same ET pathway might be utilized for the third and fourth electrons; however, the sequence of ET reactions cytochrome $c \rightarrow Cu_A \rightarrow$ binuclear site is more likely as the reduction potential of cytochrome a drops dramatically relative to Cu_A when the binuclear site is activated (Brunori et al., 1987).

CcO as a Faraday box

To incorporate the pmf and the additional conformations required for any efficient proton pump mechanism into an expanded model of the thermodynamics of redox linkage, it is necessary to predict how the potential of the various conformational states is affected by the components of the pmf, $\Delta\psi$ and $-2.303(RT/F)\Delta pH$ (Wikström and Saraste, 1984; Rottenberg, 1979). Reliable estimates of perturbations to the potentials clearly depends on an accurate assessment of how these electrostatic and pH potential gradients vary within the protein matrix. Although it is tempting to assume that an electrostatic potential difference across a membrane gives rise to a potential gradient with a simple linear dependence on distance across the membrane, this picture is only a first approximation. The higher static dielectric constant in the region of the lipid head groups relative to the center of the lipid bilayer results in a compression of the potential energy surfaces in the head group regions of the membrane. The result is that a substantial $\Delta\psi$ exists over the head group regions of the lipid bilayer. A similar compression of the potential energy surfaces is expected to occur near the surface of integral membrane proteins such as CcO as the dielectric constant near the aqueous interfaces of these proteins is expected to be larger than that in the hydrophobic core.

The Cu_A site is probably approximately 10 Å from the surface of CcO as at least one of the strictly conserved cysteines of subunit II (Cys 196 and Cys 200) is a ligand for the Cu_A site (Stevens et al., 1982), and Glu 198 is a surface residue as evidenced by labeling studies (Millett et al., 1983). In addition, another probable Cu_A ligand (His 161 of subunit II) is modified by arylazidocytochrome c, indicating that this ligand is near the protein's surface (Bisson et al., 1982). Thus, in the presence of a transmembrane potential, an electron transferred from cytochrome c to the Cu_A site likely experiences a greater potential difference than an electron transferred over a distance of 10 Å in the interior of the enzyme complex. Similarly, the energetics of proton transfers are different in various locations within the protein matrix. In this manner, the protein acts somewhat as a Faraday box shielding the hydrophobic core from external fields (clearly, the protein does not act as a true Faraday box as the surface is not a perfect conductor). It is thus expected that electron and proton transfers across the inner and outer protein surfaces of CcO require a substantial driving force so that the desired reaction occurs even in the presence of a pmf.

Energetics of the Chan Cu_A model

In the Chan Cu_A model of redox linkage, each of the states A-G denotes the conformation of the protein as a whole; in the description of the model, attention is focused more on the conformation of the linkage site. There are seven different conformational states of the Chan Cu_A model depicted in Fig. 3, and each of these states has a different oxidation potential. (It is more convenient to use oxidation potentials rather than reduction potentials in the context of the present discussion; oxidation potential = − reduction potential.)

In the absence of a pmf, the final state, $(c^{3+}A)$, is assumed to have an oxidation potential of −1060 mV as discussed earlier; that is, the oxidation potential of the oxyferryl and hydroxyl intermediates is approximately −1060 mV (the hydroxyl intermediate results from one-electron reduction of the oxyferryl intermediate). The initial state, $(c^{2+}A)$, has an oxidation potential of −250 mV. In this notation, $(c^{3+}A)$ denotes a later dioxygen intermediate than $(c^{2+}A)$. The 810-mV potential difference between these two states is the redox energy lost mostly as heat upon input of the third and fourth electrons to the enzyme. According to the Chan Cu_A model, this energy is lost in seven sequential steps. To estimate the oxidation potentials of the other six states of the Chan Cu_A model (the two possibilities involving A are discussed above), it is useful to first estimate the perturbing effect of a pmf on these potentials. The rationale for this exercise will become clear later.

For purposes of this discussion, it is assumed that a 50-mV electrostatic potential gradient exists within the first 10 Å of the inner and outer surfaces of CcO under fully energized conditions (pmf = 200 mV; $\Delta\psi$ = 150 mV; $-2.303(RT/F)\Delta pH$ = 50 mV). Thus, the remaining 20–30 Å between the electron input and output surfaces is spanned by the remaining 50 mV of the electrostatic potential. These assumptions are consistent with the above view of CcO acting somewhat as a Faraday box. As the Cu_A site is approximately 10 Å from the surface of the protein (see above), the conversion $(c^{2+}A) \rightarrow B$ must combat a 50-mV potential gradient under fully energized conditions according to these assumptions. The slight movement of the positively charged copper ion (approximately 3 Å) in the $B \rightarrow D$ conversion is actually favored in the presence of a $\Delta\psi$ as this motion occurs with the gradient. Because the distance traveled by the copper ion is so small, however, this conversion is minimally favored energetically, and, for simplicity, this conversion is assumed to be favored by approximately 10 mV in the presence of a $\Delta\psi$ = 150 mV. This assumption implies that the $B \rightarrow C$ and $C \rightarrow D$ conversions are each favored by approximately 5 mV. The reverse configurational changes are unfavored by double this amount because of the greater charge on the copper ion. Thus, the $E \rightarrow F$ and $F \rightarrow G$ conversions are each inhibited by approximately 10 mV in the presence of a $\Delta\psi$ = 150 mV. The remaining step, $D \rightarrow E$, must therefore be inhibited by 90 mV under these conditions. Note that this value assumes uptake of a matrix proton at the binuclear site upon ET to this site (as part of the dioxygen chemistry) by either a one-step

or two-step process (concomitant with or subsequent to the ET). A summary of these effects of $\Delta\psi$ = 150 mV on the various steps in the Chan Cu_A model cycle is given in Table 1 (column 2).

So far, only the effect of a pmf on the movement of electrons through the enzyme complex has been considered. The energetics of proton transfers are also perturbed by a pmf, although both $\Delta\psi$ and the pH gradient inhibit these transfer reactions. The Chan Cu_A model accounts only for the pumping of 1 H^+/e^- and thus fails to explain the 2 H^+/e^- stoichiometry expected for the third and fourth electrons as discussed earlier. For simplicity, we will assume that the Chan Cu_A model pumps 1 H^+/e^- in a direct fashion (as described in the model) and 1 H^+/e^- in an as yet unexplained indirect fashion (i.e., the ligand exchange reactions occurring at the Cu_A site also drive proton-pumping reactions at some distant site within the protein complex). (Although this proposal of an indirect mechanism is somewhat unsatisfactory due to a lack of molecular detail, other models that postulate a 2 H^+/e^- stoichiometry by direct means (Rousseau et al., 1993; Wikström et al., 1994) suffer from inefficient electron gating mechanisms as will be discussed later.) In addition, we will assume that both proton transfer reactions are similarly affected by a pmf at each step in the proton pump cycle. This latter assumption is most likely untrue but does not affect the arguments we wish to make below, and the model that we develop can be easily modified to incorporate any differences between the energetics of the direct and indirect pumping mechanisms. The first proton transfer reaction occurs in the $C \rightarrow D$ conversion. As this proton transfer reaction occurs over a distance approximately twice as far as the copper ion moves and as this motion is affected by both $\Delta\psi$ and the pH gradient, there exists an approximately 30-mV potential impeding proton transfer under fully energized conditions. The proton released in the $F \rightarrow G$ conversion is inhibited by an approximately 60 mV potential as this reaction is similar to the reverse of the electron input reaction, although it occurs over a slightly shorter distance and is affected by both $\Delta\psi$ and the pH gradient. The remaining 110 mV of the pmf therefore impedes the proton uptake reaction in $G \rightarrow (c^{3+}A)$. These effects of a pmf on the energetics of the Chan Cu_A model of proton pumping are also summarized in Table 1 (column 3). In addition, the total effect of a pmf on both the electron and proton transfer reactions is calculated for both a 1 and a 2 H^+/e^- stoichiometry (columns 4 and 5).

The oxidation potentials of the various intermediates of the Chan Cu_A model of redox linkage can now be estimated. As the electron input step, $(c^{2+}A) \rightarrow B$, is inhibited by approximately 50 mV under fully energized conditions, the oxidation potential of B is expected to be $\leq$−300 mV (= −250 mV + (−50 mV)). It is reasonable to expect at least approximately 20 mV of driving force for this reaction under fully energized conditions, so the oxidation potential of B is assigned as approximately −320 mV. The $B \rightarrow C$ conversion is minimally affected by a pmf. A driving force of approximately 30 mV is assigned to this conversion in the absence of a pmf to yield an oxidation potential for C of approximately −350 mV (= −320 mV + (−30 mV)). The remaining oxidation potentials of the states in the Chan Cu_A model are estimated in a similar manner assuming a driving force of 20–40 mV under fully energized conditions for each step and are tabulated in Table 1 (column 7). The one exception is the ET step, $D \rightarrow E$. To enforce irreversibility, the ET to the binuclear site is expected to be governed by a substantially larger driving force (here assumed to be 90 mV under energized conditions). Note that the ET reaction is expected to occur faster than the major conformational changes of the proton-pumping elements, making irreversibility of this ET necessary for efficient proton pumping. The effective oxidation potentials of the various states of the Chan Cu_A model under fully energized conditions can be calculated by accounting for the additional energy required for ET across the membrane bilayer and that required to pump 1 or 2 H^+/e^-. These effective oxidation potentials are tabulated in Table 1

TABLE 1 Estimated oxidation potentials of intermediates in the Chan Cu_A model of redox linkage

	Additional energetic requirement of:		Total energetic requirement for:		Effective oxidation potentials of intermediates					
Step	e^- movement	H^+ movement	1 H^+/e^-	2 H^+/e^-	pmf = 0		pmf = 200 mV, 1 H^+/e^-		pmf = 200 mV, 2 H^+/e^-	
					$(c^{2+}A)$	−250 mV	$(c^{2+}A)'$	−250 mV	$(c^{2+}A)''$	−250 mV
$(c^{2+}A) \rightarrow B$	50 mV		50 mV	50 mV	B	−320 mV	B'	−270 mV	B''	−270 mV
$B \rightarrow C$	−5 mV		−5 mV	−5 mV	C	−350 mV	C'	−305 mV	C''	−305 mV
$C \rightarrow D$	−5 mV	30 mV	25 mV	55 mV	D	−430 mV	D'	−360 mV	D''	−330 mV
$D \rightarrow E$	90 mV		90 mV	90 mV	E	−610 mV	E'	−450 mV	E''	−420 mV
$E \rightarrow F$	10 mV		10 mV	10 mV	F	−650 mV	F'	−480 mV	F''	−450 mV
$F \rightarrow G$	10 mV	60 mV	70 mV	130 mV	G	−820 mV	G'	−580 mV	G''	−490 mV
$G \rightarrow (c^{3+}A)$		110 mV	110 mV	220 mV	$(c^{3+}A)$	−1060 mV	$(c^{3+}A)'$	−710 mV	$(c^{3+}A)''$	−510 mV
Total:	150 mV	200 mV per H^+	350 mV	550 mV	ΔE:	−810 mV		−460 mV		−260 mV

Columns 2 and 3 summarize the approximate energetic requirements of electron and proton movement, respectively, for the conversions in column 1 (see Fig. 3) in the presence of a 200-mV pmf. Columns 4 and 5 are the estimated total energetic requirements for each step of the Chan Cu_A model assuming a 1 and a 2 H^+/e^- stoichiometry, respectively. The total energetic requirement for a 2 H^+/e^- stoichiometry is used to estimate the effective oxidation potential of the various intermediates by assuming that each step is spontaneous under these conditions (column 11); the oxidation potentials of the various intermediates when the pmf = 0 and for a 1 H^+/e^- stoichiometry are obtained by back calculation as described within the text (columns 7 and 9).

(columns 9 and 11). The conformations of the protein may be different in the presence of a pmf; this possibility is denoted by the use of primed and double-primed states.

These estimated effective oxidation potentials can be used to construct an expanded potential energy model of redox linkage mechanistically based on the Chan Cu_A model. This model is summarized in Fig. 4 and depicts the energetics of the proton pump in the absence of a pmf and under fully energized conditions in which a 1 or 2 H^+/e^- stoichiometry is assumed. Note that the energy stored during enzyme turnover is, for example, given by $(c^{3+}A)'' - (c^{3+}A) = 550$ mV. Although this number may seem strangely high for the 2 H^+/e^- ratio, it must be remembered that energy is stored by transfer of a negative charge-equivalent across $\Delta\psi$. It is thermodynamically possible for water oxidation to occur by reverse transfer of electrons across this $\Delta\psi$ (as has been shown by Wikström and co-workers (Wikström, 1988, 1989; Wikström and Morgan, 1992)). An alternative manner of interpreting this energy storage process is that ET across the membrane dielectric increases $\Delta\psi$, thereby increasing the pmf. This 550 mV of stored energy can be used for ATP synthesis; namely, the F_0F_1 ATP synthase couples the conversion $(c^{3+}A)'' \rightarrow (c^{3+}A)$ to ATP synthesis. The system can be recharged only by input of reactants, that is, by addition of a reductant (ferrocytochrome *c*) and an oxidant (dioxygen). It is simple to see from this theoretical framework that a pmf is a prerequisite for the storage of energy by enzyme turnover.

Implications of this model

It should be emphasized that the effective oxidation potentials in this model should not be taken too seriously. The large number of assumptions involved in calculation of these potentials reveals our ignorance of the detailed energetics of the proton pump. In addition, the $H_2O_2/H_2O_2^-$ and $H_2O_2^-/H_2O$ redox couples are expected to function at different potentials (Wikström, 1988; Wikström and Morgan, 1992). There are, however, a few general features that are expected to hold true for any refined model. The energies of $(c^{2+}A)$ and $(c^{3+}A)$ as well as of the respective primed and double-primed conformations are expected to be valid whenever $\Delta\psi = 150$ mV and $-2.303(RT/F)\Delta pH = 50$ mV and regardless of whether *A* corresponds to the Chan Cu_A model or any other model of redox linkage. From this B-type model of redox linkage, it is clear that $|\alpha_0 + \beta_0| > 400$ mV ($|\alpha_0 + \beta_0| = 560$ mV), the

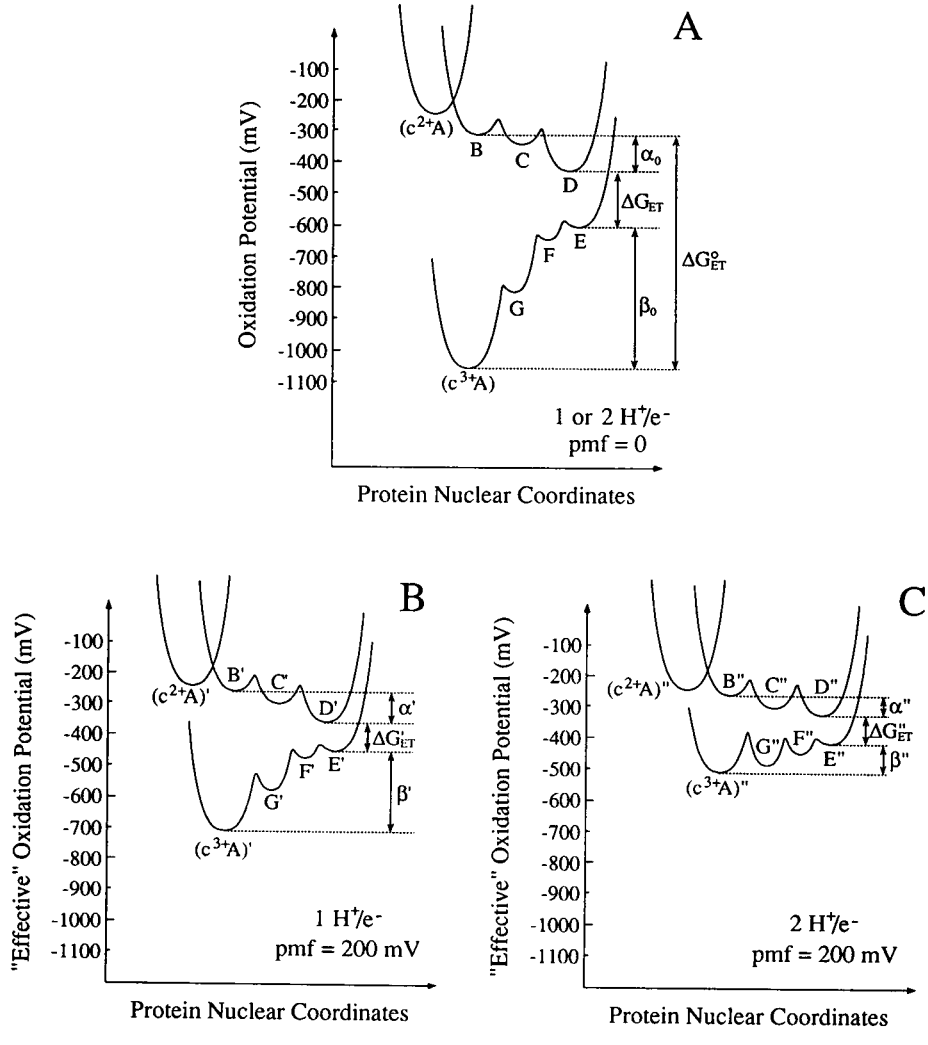

FIGURE 4 Thermodynamics of the Chan Cu_A model in an expanded model of B-type redox linkage. (*A*) depicts the energetics of the ETs and conformational changes in the absence of a membrane potential for the third and fourth electrons of the dioxygen turnover cycle. (*B*) and (*C*) reveal how these energetics are modified in the presence of a 200-mV pmf ($\Delta\psi$ = 150 mV and $-2.303(RT/F)\Delta pH = 50$ mV) assuming a 1 H^+/e^- and 2 H^+/e^- stoichiometry, respectively. Note that it is assumed here that *C* and *F* are distinct conformational states; this is not a requirement of the model, however. The values in Table 1 were used to construct this model. Note that, in the calculation of the various potentials in these schemes, we have ignored the entropic contribution to free energy that could be substantial in some steps. We expect the overall picture to remain the same, however, when this entropic contribution is included.

minimum energy needed for the pumping of 2 H^+/e^- to be spontaneous under fully energized conditions (note that, for this model, $|\alpha_0 + \beta_0|$ includes a small contribution driving electron movement within the protein complex, i.e., approximately 10 mV). Of course, this must be the case as energy is necessary to drive the conformational changes of the proton pump. The driving energies for the 1 and 2 H^+/e^- pumping stoichiometries are shown as α'/α'' and β'/β'' in Fig. 4.

This model allows an informative discussion of electron leaks and proton slips. An electron leak exists, for example, when an ET from B'' to a $(c^{3+}A)$-like state occurs (implying inefficient electron gating) instead of the desired $B'' \rightarrow C'' \rightarrow D''$ conformational change. Note that ET cannot occur from B'' to $(c^{3+}A)$ because the latter state implies that a proton or protons have been translocated. This is a subtle, but important, point. A proton slip occurs upon conversion from F'' to a $(c^{3+}A)$-like state for which the thiol proton is transferred to the tyrosinate anion or upon conversion from a C'' to a D''-like state in which the thiol proton is obtained from the intermembrane space rather than from the tyrosine. Both of these slips result from inefficient proton gating. The astute reader will note that an electron leak or a proton slip always occurs by conversion to a state of lower energy than the desired state. This is a very important point. The proton pump is successful only when a specified sequence of events occurs. Once a leak or slip occurs, the next desired conformational state is almost impossible to achieve for thermodynamic as well as kinetic reasons. Thus, in the example above, it is virtually impossible for conversion from the D''-like state to the D'' state to occur; the former state is the one of lower energy, and, mechanistically, it is straightforward to understand why this conversion does not occur. As both electron leaks and proton slips occur by conversion to a state of lower energy than the desired state, it may be somewhat difficult to understand the difference between a leak and a slip. The difference is more than just semantic because a leak occurs predominantly along the NCET whereas a slip occurs along the NCPP. We consider that this direction of the undesired conformational rearrangements or transitions defines leaks and slips.

It is important to understand why electron leaks and proton slips are more likely to occur when the pmf is large rather than when it is small. The reason for the occurrence of these undesirable reactions is that the barrier heights impeding conformational conversions in the presence of a pmf are higher than in the absence of a pmf. This fact results from the simple vertical displacement of the vibrational energy wells for a given state in the presence of a pmf. The implication of these increased barrier heights is that the turnover rate of the enzyme is necessarily slower in the presence of a pmf. This prediction agrees well with experiment (e.g., the respiratory control ratio compares the turnover rate in the absence and presence of a transmembrane potential and is typically 4–8 (Brunori et al., 1985; DiBiase and Prochaska, 1985; Antonini et al., 1991; Li et al., 1988; Steverding et al., 1990)). However, the states that give rise to leak and slip pathways are always of lower energy than those of the proton pump cycle, indicating that the barrier heights for transition to these states is almost always lower (when an electron leak is governed by a driving force in the inverted region, the barrier height for the leak may be higher than for the desired reaction). Thus, the leak and slip pathways are expected to become more favored in the presence of a pmf. This argument is not meant to imply that the proton pump does not function in the presence of a 200-mV pmf but rather that the probability that the proton pump cycle is completed is lower. Note that, as discussed above, once a leak or slip has occurred, it is virtually impossible to complete the proton pump cycle. From this analysis, we postulate that the average H^+/e^- stoichiometry is lower in the presence of a pmf. Also, the turnover rate assuming a 1 H^+/e^- stoichiometry is expected to be faster than the case for a 2 H^+/e^- stoichiometry as a result of the lower barrier heights for conformational conversion in the former case. In addition, there is a lower probability for leakage and slippage in the case of a 1 H^+/e^- stoichiometry. The enzyme may in fact be designed to utilize this 1 H^+/e^- stoichiometry pathway and mitigate the lower H^+/e^- stoichiometry via a more rapid turnover. One possible mechanism whereby this can be accomplished is if the enzyme proceeds through a $B'' \rightarrow ? \rightarrow D'$ pathway. This can be done if the energy of the D'' state becomes too high and slip occurs to the D' state (the direct or the indirect mechanism slips).

It is clear that the proton pump is coupled to the ETs to the dioxygen binding site. It is also evident that only two of the four such ETs are exergonic enough to drive the proton pump, namely the third and fourth electrons of the dioxygen reduction cycle. This fact leads to the following theoretical argument and is expected to hold for any model of the complete turnover cycle of CcO: CcO must have a mechanism preventing itself from becoming locked in a potential well of the proton pump cycle. For the first and second electrons of the dioxygen reduction cycle, the lower curves in Fig. 4 are displaced to higher energy by approximately 560 mV (the difference between the O_2/H_2O_2 and the H_2O_2/H_2O redox couples that function at approximately 500 mV and approximately 1060 mV, respectively; see above). This displacement is pictorially represented for the Chan Cu_A model under conditions in which the pmf = 0 in Fig. 5. In this model, it is clear that the conversion from B to D can occur; however, the conversion from D to $(c^{3+}A)$ cannot occur via the pathway of the Chan Cu_A model (explaining why pumping does not occur). This conversion most likely cannot occur directly either (at least in a kinetically facile manner) as the reorganizational energy (λ) for ET is so high (here, λ would include a large reorganization energy along the NCPP). The situation is even worse in the presence of a $\Delta\psi$ = 150 mV as conversion from a D-like to a $(c^{3+}A)$-like state actually becomes endergonic and λ is even greater. These arguments apply even to the simple four-state models of redox linkage in Fig. 1. Under these conditions, once the enzyme achieves the D-like configuration, turnover is essentially halted; that is, the enzyme is stuck in a potential well. The conclusion drawn from this analysis is that the enzyme must never achieve the

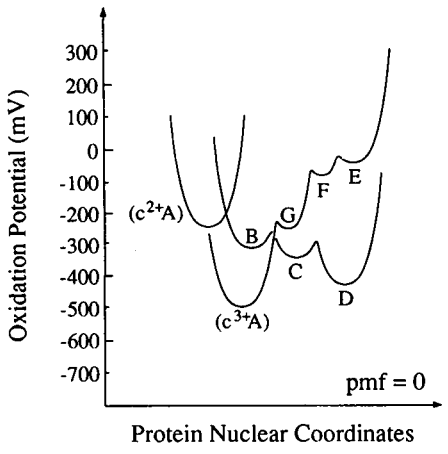

FIGURE 5 Thermodynamics of the Chan Cu_A B-type redox linkage model for the case of the first and second electrons of the dioxygen turnover cycle in the absence of a transmembrane potential. This scheme is intended to be compared with Fig. 4 *A*.

D-like conformation for the first and second electrons of the dioxygen turnover cycle. Two scenarios exist that would allow the enzyme to avoid becoming locked in a potential well: (1) the enzyme must be able to inform the linkage site as to the pumping or nonpumping nature of the incoming electrons or (2) only pumping electrons pass through the linkage site. Experiments to distinguish between these possibilities are currently in progress.

This discussion has focused on the idea that the loss of redox energy by the incoming electrons occurs in a stepwise fashion, thus providing the directionality and irreversibility required for an efficient proton pump. The proton pumping reactions occur as the protein changes its conformation to accommodate different states of varying redox energy. In other words, the change in the nuclear coordinates associated with the pumping reactions occur subsequent to the ET reactions, not concurrent with them. It is for this reason that the ET and proton pumping coordinates are separable. Note that the conformational rearrangements associated with the proton-pumping reactions are to be distinguished from the nuclear reorganizations that accompany the ET steps; the latter are small and localized at the donor and acceptor sites. Here, we assume that the coupling between the donor and acceptor sites is sufficiently weak that the ET falls within the nonadiabatic weak coupling limit of Marcus' theory (Marcus and Sutin, 1985). On the other hand, the major conformational rearrangements of the enzyme that necessarily occur globally over large distances must follow after the coupled ET reactions are completed. This is analogous to the slow conformational relaxation process that follows the rapid photoexcitation of the retinal in bacteriorhodopsin.

The proximity of cytochrome a_3 and Cu_B in the binuclear center (3–5 Å) (Brudvig et al., 1980; Chance and Powers, 1985) indicates that electron delocalization over these redox centers and any dioxygen intermediate present should be extremely fast (<1 μs). In contrast, the long-range conformational relaxations implicated in our thermodynamic model are expected to occur on a much slower time scale (micro- to milliseconds). Thus, any model that proposes cytochrome a_3 or Cu_B as the electron donor in the redox linkage step must also include a very efficient electron gating mechanism to avert uncoupled ET (electron leaks) from cytochrome a_3/Cu_B to the high potential dioxygen intermediate. None of the three models postulated to date based on the binuclear center as the site of linkage (Larsen et al., 1992; Rousseau et al., 1993; Wikström et al., 1994) has such a feature built into the model. As an illustration of this difficulty, consider Wikström's recently proposed histidine cycle model; it is difficult to understand how the $(cD^-A)_1 \rightarrow (cD^-A)_2$ relaxation can progress before the more rapid $(cD^-A)_1 \rightarrow (cDA^-)_1$ transition occurs (ET from Cu_B to the dioxygen intermediate). These arguments follow logically from sound physicochemical principles. The strong electronic coupling between Cu_B and the dioxygen intermediate anchored on cytochrome a_3 indicates that the ET that has been postulated in these models must occur in the adiabatic limit. Accordingly, these models do not provide efficient redox linkage.

CONCLUSIONS

The proton pump function of CcO dictates that this enzyme must be conformationally flexible. Specifically, reduction or oxidation of the linkage site commences a conformational relaxation process. The energy released by adoption of a more stable protein conformation is used to translocate protons against a transmembrane electrochemical gradient. As a result of this conformational cycling, the free energy of the internal ET between the linkage site and the activated binuclear center (ΔG_{ET}) is much less than that predicted from a simple difference of reduction potentials. Unfortunately, there are many undesirable configurations that the enzyme could adopt in its conformational cycling that are lower in energy than the next desired conformation. Clearly, to accomplish the desired result, kinetic barriers must be introduced to inhibit the uncoupling reactions from occurring. Thus, the existence of efficient electron and proton gating mechanisms is crucial for preventing electron leaks and proton slips from occurring during turnover. In the context of the model presented herein, electron gating mechanisms favor conformational relaxation along the NCPP until the appropriate time in the proton pump cycle for ET to occur. Proton slips occur along the NCPP but they are always more exergonic than the desired reaction. Thus, highly effective proton gating mechanisms are required for completion of the desired result with high probability. As efficient electron and proton gating mechanisms are so vital to the success of the proton pump, they are expected to be important features of any detailed model of the proton pumping process in CcO. Our analysis indicates that at high pmf enzyme turnover is expected to decrease as a result of the higher energetic barriers for ET and protein conformational changes. Therefore, it is unnecessary to invoke pmf-induced conformational changes to explain the slower experimentally observed turnover under these conditions. It is possible that a high pmf

stretches the electron and proton gating mechanisms to the limit of their effectiveness, leading to the occurrence of more energetically favorable electron leak and proton slip reactions and a reduced H^+/e^- stoichiometry. Finally, it is important to point out that CcO acts as a cooperative unit such that conformational changes occurring at a given redox center do not a priori identify that site as the site of linkage.

Special thanks to Dr. Theodore J. DiMagno and Michael H. B. Stowell for stimulating discussions that aided in the development of the model presented herein.

This work was contribution 9016 from the Division of Chemistry and Chemical Engineering, California Institute of Technology. This work was supported by grant GM22432 from the National Institute of General Medical Sciences, U. S. Public Health Service (S.I.C.). S.M.M. is a recipient of a National Research Service predoctoral award.

REFERENCES

Antonini, G., F. Malatesta, P. Sarti, and M. Brunori. 1991. Control of cytochrome oxidase activity. *J. Biol. Chem.* 266:13193–13202.

Babcock, G. T., and P. M. Callahan. 1983. Redox-linked hydrogen bond strength changes in cytochrome *a*: implications for a cytochrome oxidase proton pump. *Biochemistry.* 22:2314–2319.

Babcock, G. T., and M. Wikström. 1992. Oxygen activation and the conservation of energy in cell respiration. *Nature.* 356:301–309.

Bisson, R., G. C. M. Steffens, R. A. Capaldi, and G. Buse. 1982. Mapping of the cytochrome *c* binding site on cytochrome *c* oxidase. *FEBS Lett.* 144:359–363.

Blair, D. F., W. R. Ellis Jr., H. Wang, H. B. Gray, and S. I. Chan. 1986. Spectroelectrochemical study of cytochrome *c* oxidase: pH and temperature dependences of the cytochrome potentials. *J. Biol. Chem.* 261:11524–11537.

Bowler, B., A. L. Raphael, and H. B. Gray. 1990. Long-range electron transfer in donor (spacer) acceptor molecules and proteins. *In* Progress in Inorganic Chemistry: Bioinorganic Chemistry, Vol. 38. S. J. Lippard, editor. John Wiley and Sons, New York. 259–319.

Brezezinski, P., and B. G. Malmström. 1987. The mechanism of electron gating in proton pumping cytochrome *c* oxidase: the effect of pH and temperature on internal electron transfer. *Biochim. Biophys. Acta.* 894: 29–38.

Brudvig, G. W., T. H. Stevens, and S. I. Chan. 1980. Reactions of nitric oxide with cytochrome *c* oxidase. *Biochemistry.* 19:5275–5285.

Brunori, M., G. Antonini, A. Colosimo, F. Malatesta, P. Sarti, M. G. Jones, and M. T. Wilson. 1985. Stopped-flow studies of cytochrome oxidase reconstituted into liposomes: proton pumping and control of activity. *J. Inorg. Chem.* 23:373–379.

Brunori, M., G. Antonini, F. Malatesta, P. Sarti, and M. T. Wilson. 1987. Structure and function of cytochrome oxidase: a second look. *Adv. Inorg. Biochem.* 7:93–154.

Calhoun, M. W., J. W. Thomas, and R. B. Gennis. 1994. The cytochrome oxidase superfamily of redox-driven proton pumps. *Trends Biochem. Sci.* 19:325–330.

Casey, R. P., M. Thelen, and A. Azzi. 1979. Dicyclohexylcarbodiimide inhibits proton translocation by cytochrome *c* oxidase. *Biochem. Biophys. Res. Commun.* 87:1044–1051.

Chan, S. I., and P. M. Li. 1990. Cytochrome *c* oxidase: understanding nature's design of a proton pump. *Biochemistry.* 29:1–12.

Chance, B., and L. Powers. 1985. Structure of cytochrome oxidase redox centers in native and modified forms: an EXAFS study. *Curr. Top. Bioenerg.* 14:1–19.

DiBiase, V. A., and L. J. Prochaska. 1985. Characterization of electron-transfer and proton translocation activities in trypsin-treated bovine heart michondrial cytochrome *c* oxidase. *Arch. Biochem. Biophys.* 243:668–677.

Fabian, M., P.-E. Thörnström, P. Brezezinski, and B. G. Malmström. 1987. Two-electron reduction is required for rapid internal electron transfer in resting, pulsed and oxygenated cytochrome *c* oxidase. *FEBS Lett.* 213: 396–400.

Gelles, J., D. F. Blair, and S. I. Chan. 1986. The proton-pumping site of cytochrome *c* oxidase: a model of its structure and mechanism. *Biochim. Biophys. Acta.* 853:205–236.

Hill, B. C. 1991. The reaction of the electrostatic cytochrome *c*-cytochrome *c* oxidase complex with oxygen. *J. Biol. Chem.* 266:2219–2226.

Hill, B. C. 1994. Modeling the sequence of electron transfer reactions in the single turnover of reduced, mammalian cytochrome *c* oxidase with oxygen. *J. Biol. Chem.* 269:2419–2425.

Larsen, R. W., L.-P. Pan, S. M. Musser, Z. Li, and S. I. Chan. 1992. Could Cu_B be the site of redox linkage in cytochrome *c* oxidase? *Proc. Natl. Acad. Sci. USA.* 89:723–727.

Li, P. M., J. E. Morgan, T. Nilsson, M. Ma, and S. I. Chan. 1988. Heat treatment of cytochrome *c* oxidase perturbs the Cu_A site and affects proton pumping behavior. *Biochemistry.* 27:7538–7546.

Malmström, B. G. 1990. Cytochrome *c* oxidase as a redox-linked proton pump. *Chem. Rev.* 90:1247–1260.

Malmström, B. G. 1994. Rack-induced bonding in blue-copper proteins. *Eur. J. Biochem.* 223:711–718.

Marcus, R. A., and N. Sutin. 1985. Electron transfers in chemistry and biology. *Biochim. Biophys. Acta.* 811:265–322.

Millett, F., C. de Jong, L. Paulson, and R. A. Capaldi. 1983. Identification of the specific carboxylate groups on cytochrome *c* oxidase that are involved in binding cytochrome *c*. *Biochemistry.* 22:546–552.

Musser, S. M., M. H. B. Stowell, and S. I. Chan. 1993a. Comparison of ubiquinol and cytochrome *c* terminal oxidases. *FEBS Lett.* 327:131–136.

Musser, S. M., M. H. B. Stowell, and S. I. Chan. 1993b. Futher comparison of ubiquinol and cytochrome *c* terminal oxidases. *FEBS Lett.* 335:296–298.

Myslovatyi, B. S., D. L. Zairov, A. A. Chebotarev, and É. L. Muzykantskii. 1982. Partial pressure of oxygen in different organs and tissues and some hemodynamic parameters in tourniquet shock. *Bull. Exp. Biol. Med.* 94: 872–875.

Oliveberg, M., and B. G. Malmström. 1991. Internal electron transfer in cytochrome *c* oxidase: evidence for a rapid equilibrium between cytochrome *a* and the bimetallic site. *Biochemistry.* 30:7053–7057.

Pan, L.-P., J. T. Hazzard, J. Lin, G. Tollin, and S. I. Chan. 1991. The electron input to cytochrome *c* oxidase from cytochrome *c*. *J. Am. Chem. Soc.* 113:5908–5910.

Proteau, G., J. M. Wrigglesworth, and P. Nicholls. 1983. Protonmotive functions of cytochrome *c* oxidase in reconstituted vesicles. *Biochem. J.* 210:199–205.

Rodkey, F. L., and E. G. Ball. 1950. Oxidation-reduction potentials of the cytochrome *c* system. *J. Biol. Chem.* 182:17–28.

Rottenberg, H. 1979. The measurement of membrane potential and ΔpH in cells, organelles, and vesicles. *Methods Enzymol.* 55:547–569.

Rousseau, D. L., Y.-C. Ching, and J. Wang. 1993. Proton translocation in cytochrome *c* oxidase: redox linkage through proximal ligand exchange on cytochrome a_3. *J. Bioenerg. Biomembr.* 25:165–176.

Sigel, E., and E. Carafoli. 1979. The charge stoichiometry of cytochrome *c* oxidase in the reconstituted system. *J. Biol. Chem.* 254:10572–10574.

Solioz, M., E. Carafoli, and B. Ludwig. 1982. The cytochrome *c* oxidase of *Paracoccus denitrificans* pumps protons in a reconstituted system. *J. Biol. Chem.* 257:1579–1582.

Stevens, T. H., C. T. Martin, H. Wang, G. W. Brudvig, C. P. Scholes, and S. I. Chan. 1982. The nature of Cu_A in cytochrome *c* oxidase. *J. Biol. Chem.* 257:12106–12113.

Steverding, D., B. Kadenbach, N. Capitanio, and S. Papa. 1990. Effect of chemical modification of lysine amino-groups on redox and proton motive activity of bovine heart cytochrome *c* oxidase reconstituted in phospholipid-membranes. *Biochemistry.* 29:2945–2950.

Stowell, M. H. B., R. W. Larsen, J. R. Winkler, D. C. Rees, and S. I. Chan. 1993. Transient electron-transfer studies on the two-subunit cytochrome *c* oxidase from *Paracoccus denitrificans*. *J. Phys. Chem.* 97:3054–3057.

Trumpower, B. L., and R. B. Gennis. 1994. Energy transduction by cytochrome complexes in mitochondrial and bacterial respiration: the enzymology of coupling electron transfer reactions to transmembrane proton translocation. *In* Annual Review of Biochemistry, Vol. 63. C. C. Richardson, J. N. Abelson, A. Meister, and C. T. Walsh, editors. Annual Reviews, Inc., Palo Alto, CA. 675–716.

van der Oost, J., A. P. N. de Boer, J.-W. L. de Gier, W. G. Zumft, A. H. Stouthamer, and R. J. M. van Spanning. 1994. The heme-copper oxidase family consists of three distinct types of terminal oxidases and is related to nitric oxide reductase. *FEMS Micro. Biol. Lett.* 121:1–10.

van Verseveld, H. W., K. Krab, and A. H. Stouthamer. 1981. Proton pump coupled to cytochrome *c* oxidase in *Paracoccus denitrificans*. *Biochim. Biophys. Acta.* 635:525–534.

Wang, H., D. F. Blair, W. R. Ellis Jr., H. B. Gray, and S. I. Chan. 1986. Temperature dependence of the reduction potential of Cu_A in carbon monoxide inhibited cytochrome *c* oxidase. *Biochemistry.* 25:167–171.

Wikström, M. K. F. 1977. Proton pump coupled to cytochrome *c* oxidase in mitochondria. *Nature.* 266:271–273.

Wikström, M. 1988. Mechanism of cell respiration. *Chemica Scripta.* 28A: 71–74.

Wikström, M. 1989. Identification of the electron transfers in cytochrome oxidase that are coupled to proton-pumping. *Nature.* 338:776–778.

Wikström, M., A. Bogachev, M. Finel, J. E. Morgan, A. Puustinen, M. Raitio, M. Verkhovskaya, and M. I. Verkhovsky. 1994. Mechanism of proton translocation by the respiratory oxidases: the histidine cycle. *Biochim. Biophys. Acta.* 1187:106–111.

Wikström, M., and J. Morgan. 1992. The dioxygen cycle. *J. Biol. Chem.* 267:10266–10273.

Wikström, M., and M. Saraste. 1984. The mitochondrial respiratory chain. *In* Bioenergetics, Vol. 9. L. Ernster, editor. Elsevier, Amsterdam. 49–94.

Wikström, M. K. F., and K. Krab. 1978. Cytochrome *c* oxidase is a proton pump. *FEBS Lett.* 91:8–14.

Williams, R. J. P. 1990. Overview of biological electron-transfer. *In* Electron Transfer in Biology and the Solid State, Vol. 226. M. K. Johnson, R. B. King, D. M. Kurtz Jr., C. Kurtal, M. L. Norton, and R. A. Scott, editors. American Chemical Society, Washington, DC. 3–23.

Woodruff, W. H. 1993. Coordination dynamics of heme-copper oxidases: the ligand shuttle and the control and coupling of electron transfer and proton translocation. *J. Bioenerg. Biomembr.* 25:177–188.